Thermal Penetration of Gold Nanoparticles into Silicon Dioxide

I. Ilkiv[a,*], K. Kotlyar[a], D. Amel'chuk[b], S. Lebedev[b], G. Cirlin[a,c,d,e]
and A. Bouravleuv[a,b,d]

[a]St. Petersburg Academic University, Khlopina Str. 8/3, 194021 St. Petersburg, Russia
[b]Ioffe Physicotechnical Institute, Politekhnicheskaya Str. 26, 194021 St. Petersburg, Russia
[c]ITMO University, Kronverkskiy Pr. 49, 197101 St. Petersburg, Russia
[d]Institute for Analytical Instrumentation, RAS, Rizhsky Str. 26, 190103 St. Petersburg, Russia
[e]Peter the Great St. Petersburg Polytechnic University, Polytechnicheskaya Str. 29, 195251 St. Petersburg, Russia

We report on an experimental study of the thermal annealing processes under air and nitrogen atmospheres of colloidal Au nanoparticles deposited onto $SiO_2/Si(100)$ samples. It was shown that Au nanoparticles during annealing under ambient conditions could penetrate inside silicon dioxide layers forming pores at that their lengths were found to be dependent on the annealing time. The influence of oxygen on the penetration process is discussed. At the same time, the annealing of Au nanoparticles under nitrogen conditions did not result in the formation of pores.

1. Introduction

Noble metallic nanoparticles (NPs) with diameter smaller than 100 nm are attractive materials due to their original and tunable properties compared with their bulk counterparts [1]. Among them, monodispersed Au NPs in solutions attract particular attention due to their stability and ease of synthesis. Au NPs are of great interest for the nanotechnologies, biomedicine, biotechnologies, the catalysis reactions. In particular, Au NPs have been used for creation sensors based on surface plasmon resonance [2], the reduction of carbon dioxide [3], various electronic applications [4], the synthesis of nanoporous membranes [5] and the vapor–liquid–solid (VLS) growth of semiconductor nanowires [6].

At the same time, Au NPs can be encapsulated in dielectric matrices (e.g. polymers, silicon dioxide, oxynitride layers, etc.) for creation of the nanocomposite films, which are of importance because of their unusual nonlinear optical and electrical properties [7, 8]. Evidently, the properties of nanocomposites will depend on the size, density, and the position of Au NPs [9]. Nowadays these nanocomposites can be fabricated using several technological approaches, such as the sol–gel process, metal–dielectric co-sputtering deposition, metal–ion implantation of dielectrics and *in situ* growth [10–13]. Nevertheless, they cannot guarantee the homogeneous size distribution of NPs, as well as their spatial arrangement, especially for the samples with a large surface area.

It was recently shown that Au nanoparticles deposited on the SiO_2/Si and annealed under certain conditions were penetrated inside SiO_2 [14]. In fact, this is a promising method, which can be used for a low cost nanopatterning and nanocomposite materials fabrication mentioned above, because of its easy manufacturing. At the same time, this process is quite complicated; some important unanswered questions remain open and wait for the appropriate explanations. Therefore, investigation of Au NP behavior on sample surfaces at enhanced temperatures is important not only from the viewpoint of fundamental issues, but also for the diverse practical applications.

Here we report on an experimental study of the thermal annealing processes of colloidal Au nanoparticles deposited on the SiO_2 surface under both air and nitrogen atmospheres.

2. Experimental details

The deposition of Au colloidal solutions was performed onto the Si(100) substrates with preliminary created by thermal oxidation 190 nm thick SiO_2 layers. Prior to the deposition, the surface of the samples was modified by a short time Ar plasma treatment, which resulted in a global improvement of the NP adhesion and the hydrophilic properties of the sample surfaces. Colloidal Au NPs solutions were supplied by BBI Solutions, UK. We used Au NPs having 40 nm nominal diameter. The solution remnants were blown away with a dry N_2 gas.

The heat treatment of the samples with deposited Au nanoparticles was carried out in the horizontal furnace under ambient air, whereas they were loaded into an already heated furnace. After the treatment, the samples were cooled down passively to room temperature inside the oven.

---

*corresponding author; e-mail: fiskerr@ymail.com

The morphological properties of samples were investigated using a scanning electron microscope (SEM) Zeiss Supra 25 operating at 20 kV.

3. Results and discussion

First, the deposition of colloidal Au NPs was performed onto SiO_2/Si for 150 s. The SEM image of the sample surface with the deposited colloidal Au NPs is shown in Fig. 1. Au NPs are distributed randomly, but rather homogeneously across the whole sample surface. The average surface density of NPs is about 8×10^7 cm^{-2}.
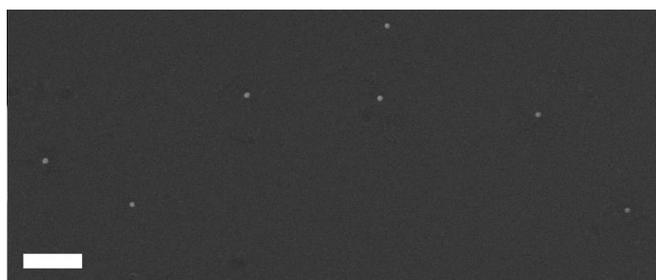

Fig. 1. SEM image of the sample surface after the colloidal Au NP solution deposition for 150 s. Scale bar corresponds to 400 nm.
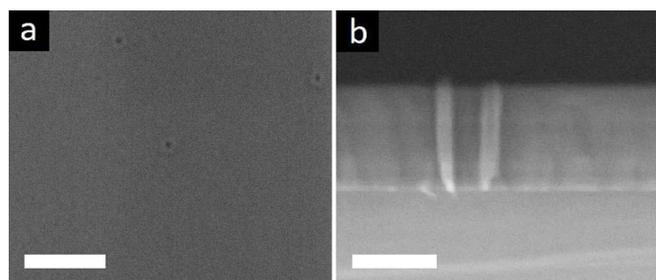

Fig. 2. SEM image of the sample surface after the thermal annealing for 100 min under ambient air: (a) top view, (b) cross-sectional view of the cleaved sample. Scale bars correspond to 200 nm.
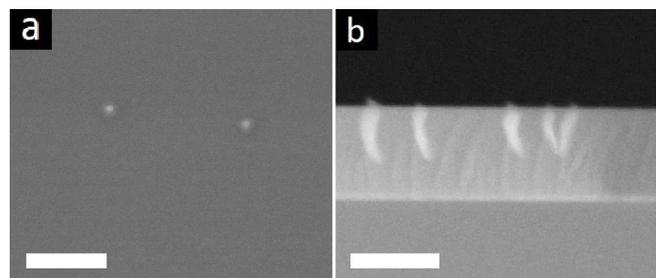

Fig. 3. As in Fig. 2, but for thermal annealing for 25 min.

After the thermal annealing under ambient conditions for 100 min at 1000 °C in a horizontal furnace, the formation of circle holes was observed on the sample surface (see Fig. 2). The surface density of holes was in a good agreement with the density of Au NPs. For the more detailed study of samples, they were cleaved and SEM investigation of the sample cross-sections was performed. The results obtained are shown in Fig. 2. It seems that during the annealing Au NPs were penetrated inside SiO_2 layer towards Si/SiO_2 interface forming the channels or pores. Their orientation was generally normal to the surface (Fig. 2b). Despite the Au NP diameters were equal to 40 nm, the pore diameters decreased to 20 nm. The similar results have been recently demonstrated in [14, 15]. Moreover, it seems that at an initial stage of the penetration process the formation of ridges around Au NPs took place (Fig. 2a).

Taking into account results obtained, we assumed that the Au NP penetration mechanism might be connected with the redox reaction. It is well known that in ultra-high vacuum (UHV) the decomposition temperature of the SiO_2 layer usually varies from 800 to 1000 °C. Au NPs deposited onto the SiO_2 surface can play a role of a catalyst for the decomposition reaction lowering the temperature of SiO_2 destruction to 600–700 °C [15]. The SiO_2 decomposition seems to occur selectively under the Au NPs, because of the pore creation due to formation of volatile SiO as a result of the following reaction: $SiO_2 + Si = 2SiO$ [16, 17]. The thermal annealing of Au NPs under ambient air, i.e. with the possibility of additional oxidation, apparently change the process of SiO_2 decomposition. In this case, the reverse redox reaction can occur. The walls of the created channels can be additionally oxidized, i.e. narrowing the pores. When Au NPs reach Si/SiO_2 interface, the rates of decomposition and the precipitation reaction can be balanced and the penetration can be stopped. At the same time, at the initial stage of decomposition, Au NPs appeared to form the liquid droplets, which wetted the samples surface. It is known that the decomposition process occurred more effectively under the droplets, because of strong NP support interactions [18]. At that, an additional oxidation takes place at the triple point line around the droplet forming the ridge. When the droplets started to penetrate into dioxide overlayer, its surface area shrinks out. Therefore, the pore diameters are smaller than ridges ones (see Fig. 2a). As it was already mentioned, the controls under the depth of NP penetration inside the dielectric matrix are of the importance for many possible device applications. Evidently, that depth should depend on the annealing time. Therefore, in order to change the Au NP penetration depth we performed additional investigations with smaller times of annealing. SEM study of the samples annealed for 50 min did not show any significant differences.

The more interesting results were observed for the 25 min treated sample (see Fig. 3). The bright spots can be seen in the centers of ridges, which are related to gold visibility due to the small depth of Au NP embedding (Fig. 3a). At the same time, the samples annealed for a longer times (Fig. 2a) exhibited the dark spots, which can be caused by the formation of halls as a result of

Au NP penetration into the SiO_2 layer. The SEM investigations of the cleaved samples allowed to determine the lengths of the pores, which were equaled to 120 nm (Fig. 3b). Therefore, Au NPs penetrated into SiO_2 at velocity of about 5 nm/min. Thus, Au NPs would reach the Si/SiO_2 interface after 38 min of annealing and then penetration process can be stopped.

In order to check the importance of oxygen in the processes, we carried out the rapid thermal annealing (RTA) of the Au NPs in the atmosphere of nitrogen. The samples were annealed under N_2 flow rate of 500 cc/min for 60 min at temperature of 940 °C. It was found that the Au NPs kept their initial position during the thermal annealling. The Au NPs changed their forms from a spherical to the hexagonal only. It seems that in the nitrogen atmosphere Au NPs, due to the absorbance of some Si adatoms as a result of destruction of SiO_2 overlayer, there can form Si_xN_y layer [19, 20] stopping the destruction and penetration processes. Thus, the additional control under the penetration of Au NPs seems to be achieved by changing of ambient to nitrogen conditions during the annealing of the samples.

4. Conclusions

In summary, we performed an experimental study of Au NP behavior on the SiO_2 surface during thermal annealing at temperatures up to 1000 °C under different ambient conditions. The result obtained revealed that Au NPs during annealing under ambient air can penetrate into SiO_2 forming pores with lengths depending on the time of annealing. The formation of pores occurs due to Au-assisted redox reactions. At the same time, annealing under nitrogen seemed led to nitridation of the sample surfaces. The easy manufacturing procedure and controllability of the present method can find many potential applications for the fabrication of opto- and nanoelectronic devices.

Acknowledgments

References

[1] B.R. Cuenya, F. Behafarid, *Surf. Sci. Rep.* **70**, 135 (2015).

[2] L.A. Austin, M.A. Mackey, E.C. Dreaden, M.A. El-Sayed, *Arch. Toxicol.* **88**, 1391 (2014).

[3] W. Zhu, R. Michalsky, Ö. Metin, Lv. Haifeng, S. Guo, C.J. Wright, X. Sun, A.A. Peterson, S. Sun, *J. Am. Chem. Soc.* **135**, 1683345 (2013).

[4] H.H. Hsieh, Y.M. Sung, F.C. Hsu, K.J. Hsiao, Y.J. Lee, Y.F. Chen, *RSC Adv.* **5**, 1549 (2015).

[5] L.J. De Vreede, M.S. Muniz, A. Van den Berg, J.C.T. Eijkel, *J. Micromech. Microeng.* **26**, 037001 (2016).

[6] R. Jafari Jam, M. Heurlin, V. Jain, A. Kvennefors, M. Graczyk, I. Maximov, M.T. Borgström, H. Pettersson, L. Samuelson, *Nano Lett.* **15**, 134 (2014).

[7] H. Liao, W. Wen, G.K. Wong, *JOSA B* **23**, 2518 (2006).

[8] J.L. Gu, J.L. Shi, G.J. You, L.M. Xiong, S.X. Qian, Z.L. Hua, H.R. Chen, *Adv. Mater.* **17**, 557 (2005).

[9] P.K. Jain, K.S. Lee, I.H. El-Sayed, M.A. El-Sayed, *J. Phys. Chem. B* **110**, 7238 (2006).

[10] W.T. Wang, Z.H. Chen, G. Yang, D.Y. Guan, G.Z. Yang, Y.L. Zhou, H.B. Lu, *Appl. Phys. Lett.* **83**, 1983 (2003).

[11] D. Dalacu, L. Martinu, *Appl. Phys. Lett.* **77**, 4283 (2000).

[12] V. Pardo-Yissar, R. Gabai, A.N. Shipway, T. Bourenko, I. Willner, *Adv. Mater.* **13**, 1320 (2001).

[13] S. Dhara, R. Kesavamoorthy, P. Magudapathy, M. Premila, B.K. Panigrahi, K.G.M. Nair, C.T. Wu, K.H. Chen, L.C. Chen, *Chem. Phys. Lett.* **370**, 254 (2003).

[14] L.J. de Vreede, A. van den Berg, J.C.T. Eijkel, *Nano Lett.* **15**, 727 (2015).

[15] V.S. Gerasimov, A.E. Ershov, A.P. Gavrilyuk, S.V. Karpov, H. Ăgren, S.P. Polyutov, *Opt. Expr.* **24**, 26851 (2016).

[16] P. Babor, R. Duda, J. Polcak, S. Prusa, M. Potocek, P. Varga, J. Cechal, T. Sikola, *RSC Adv.* **5**, 101726 (2015).

[17] Y. Enta, T. Naga, T. Yoshida, N. Ujiie, H. Nakazawa, *J. Appl. Phys.* **114**, 114104 (2013).

[18] M. Ahmadi, H. Mistry, B. Roldan Cuenya, *J. Phys. Chem. Lett.* **7**, 3519 (2016).

[19] W. Orellana, *Appl. Phys. Lett.* **84**, 933 (2004).

[20] H.K. Sanghera, J.L. Sulliva, *Surf. Interf. Anal.* **27**, 678 (1999).